Adaptive Control for a Mobile Robot Under Slip Conditions Using an LMI-Based Approach

Article *in* European Journal of Control · December 2010

DOI: 10.3166/ejc.16.144-155

European Journal of Control (2010)2:144–155

DOI:10.3166/EJC.16.144–155

European Journal of Control

Adaptive Control for a Mobile Robot Under Slip Conditions Using an LMI-Based Approach

Ramon Gonzalez[1]*, Mirko Fiacchini[2], Teodoro Alamo[2], Jose Luis Guzman[1], Francisco Rodriguez[1]

[1]Departamento de Lenguajes y Computación, University of Almería, Almería, Spain;
[2]Departamento de Ingeniería de Sistemas y Automática, University of Seville, Seville, Spain

This paper presents a control law for the trajectory tracking of mobile robots under slip conditions and subject to both system constraints and varying dynamics. First, a control law is obtained based on a Lyapunov function to guarantee closed-loop asymptotic stability, resulting in a set of feedback gains, one for each extreme model realization. On-line computation is devoted to determine an adaptive feedback control law for the current realization of the state as a convex combination of the gains previously obtained. Simulations comparing the proposed control law with other strategies under slip conditions are provided. They show the satisfactory behavior of the proposed control strategy.

Keywords: Adaptive control, autonomous mobile robot, linear matrix inequalities, slip

1. Introduction

Mobile robot control systems must deal with both state and input constraints, i.e. physical limitations of actuators, non-holonomic constraints, narrow work-space, etc. Furthermore, mobile robots constitute non-holonomic systems, which cannot by stabilized by smooth static state feedback laws [8]. These systems fail in the *Brockett's Condition* for the existence of a continuously differentiable control law, as the dimension of the state space is three and the number of control signals is only two [6]. In order to solve this problem, discontinuous feedback control laws [4] and adaptive continuous feedback control laws have been commonly used [9, 20, 26].

On the other hand, mobile robots operating on off-road conditions present some phenomena as slip or sliding which cause that rolling of a wheel is not perfect [31]. Thereby, the guidance and the controllability of the mobile robot is considerably influenced by the condition of terrain [13]. For that reason, one key issue is to design motion controllers that compensate slip effects. For example, a study for four generic wheeled mobile robots in the presence of wheel skidding and slipping from a control perspective is developed in [30]. Disturbances due to skidding and slipping are categorically classified as input-additive, input-multiplicative, and/or matched/unmatched perturbations. A linear feedback control law for a Tracked Mobile Robot (TMR) is presented in [13], where gains are adapted according to the longitudinal slip measured in real-time. In [10, 21], the problem is addressed for an Ackermann-type agricultural vehicle in which adaptive and predictive control techniques are used to face the lateral slip effects. The work presented in [22] proposes a control for a TMR based on a kinematic approach using the different values of the instantaneous rotation center (IRC) of the tracks.

**Correspondence to:* R. Gonzalez, E-mail: rgonzalez@ual.es

Received 1 June 2009; Accepted 16 October 2009
Recommended by A. Astolfi, A.J. van der Schaft

The IRC position depends on the track–soil interactions.

This paper focuses on the synthesis of an adaptive control law, which guarantees asymptotic stability for a linear, time-varying, discrete-time system subject to both constraints and varying dynamics. The constraints are imposed supposing that the mobile robot operates in narrow spaces as the actuators are physically saturated. The objective is to determine an adaptive control law and a Lyapunov function guaranteeing the asymptotic stability of the closed-loop system. We formulate the problem in terms of Linear Matrix Inequalities (LMI) optimization problem [5, 17], in order to obtain a positive definite matrix P determining the Lyapunov function, and a set of feedback gains composing the control law. This problem is solved off-line for each extreme realizations of the system dynamics. Afterwards, an on-line adaptive feedback control law is used depending on the current system realization. This adaptive control law is obtained as a convex combination of the previously determined gains.

It is important to remark that the control law presented here tries to compensate the slip effect, considering the slip in the control design. An interesting alternative is to include a velocity/acceleration limiter that would prevent the robot's wheel from slip [16, 25]. However, as discussed in [31], this solution could become unsuitable in practice. The reason is that off-road terrains are intrinsically loose, producing a non-controllable slip, that is, the robot will slip although velocity and acceleration are limited.

LMI-based solutions have been satisfactorily applied in other mobile robotics problems. For instance, backing control of simulated mobile robots with multiple trailers by fuzzy modelling and control is presented in [29]. LMI are used to solve the problem of finding stable feedback gains and a common Lyapunov function. In [1], a feedback path controller for an articulated mining vehicle based on LMI techniques to guarantee stability of the closed-loop system is proposed. In [32], a robust tracking problem of wheeled mobile robots subject to non-holonomic constraints and input constraints is discussed. In the framework of LMI, the suggested tracking scheme is formulated as an on-line controller, which is obtained solving a constrained H_∞ control law. The work [23] shows a method for motion planning of mobile robots. The free configuration space is decomposed into Delaunay triangles, and an optimum channel from initial to goal configurations is found by solving an LMI system.

The paper is organized as follows: a modification of the standard kinematic model including slip effects, and the trajectory tracking error model, is presented in Section 2. Section 3 is devoted to obtain the adaptive control law using the LMI-based approach to guarantee stability under input and state constraints. Simulations of the proposed control law with other control strategies are detailed in Section 4. Finally, conclusions and future trends are summarized in Section 5.

2. Trajectory Tracking Based on Kinematic Model with Slip

In this section, we present a modified formulation of the well-known kinematic model of a differential-drive wheeled mobile robot [7, 28]. For that purpose, this kinematic model has been extended with a parameter, which weighs the slip factor of the terrain [13]. In this case, we suppose that the mobile robot will operate at low velocities, and we only consider longitudinal slip. As stated in [15, 19, 27], lateral slip is zero for straight line motions and it can be neglected when the vehicle turns "on the spot" or at low velocities. However, longitudinal slip is an unavoidable effect of pneumatic tire compression/reaction to soil shearing due to the own characteristics of wheeled/tracked locomotion [13, 30, 31].

Furthermore, the trajectory-tracking or posture-tracking problem is also described and the error state space system is obtained using the modified kinematic model.

2.1. Kinematic Model under slip conditions

When wheel slip is not considered, the linear velocity of the wheels is [28]

$$\begin{aligned} v_r(t) &= \rho\phi_r(t), \\ v_l(t) &= \rho\phi_l(t), \end{aligned} \tag{1}$$

where $t \in \mathbb{R}$ is the continuous time, ρ is the wheel (or track), rolling radius, and v_r/ϕ_r and v_l/ϕ_l are the linear/angular velocities of the right and left wheels respectively.

As commented above, (longitudinal) slip can be considered as a penalizing factor of the wheel velocity [13, 31]

$$\begin{aligned} v_r^{slip}(t) &= \rho\phi_r(t)\,(1 - i_r(t)), \\ v_l^{slip}(t) &= \rho\phi_l(t)\,(1 - i_l(t)), \end{aligned} \tag{2}$$

where i_r and i_l are the terms representing the (longitudinal) slip component of each wheel on a terrain. As shown in [13], slip can be estimated in real-time using the appropriate sensors.

Using this knowledge in the classical kinematic model of a differential-drive robot [28], we obtain

$$\dot{x}(t) = \frac{v_r(t)(1 - i_r(t)) + v_l(t)(1 - i_l(t))}{2}\cos\theta(t),$$
$$\dot{y}(t) = \frac{v_r(t)(1 - i_r(t)) + v_l(t)(1 - i_l(t))}{2}\sin\theta(t),$$
$$\dot{\theta}(t) = \frac{v_r(t)(1 - i_r(t)) - v_l(t)(1 - i_l(t))}{b}, \tag{3}$$

where $[x \quad y \quad \theta]^T$ represents the location (position and orientation) of the mobile robot, and b is the distance between the wheels' centers.

2.2. Trajectory tracking error model

Trajectory tracking problem can be seen as a problem in which a robot must follow a *virtual mobile robot* representing the desired positions and velocities, as shown in Fig. 1. Hence, the objective is to find a feedback control law [8, 12]

$$\nu(t) = (v_r(t), v_l(t)) = f(p(t), p^{ref}(t), v_r^{ref}(t), v_l^{ref}(t)), \tag{4}$$

such that

$$\lim_{t\to\infty} e(t) = \lim_{t\to\infty} [p^{ref}(t) - p(t)] = 0, \tag{5}$$

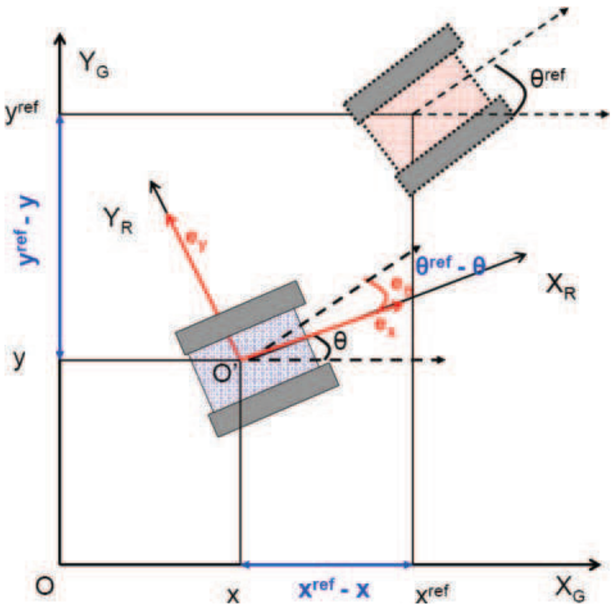

Fig. 1. Graphical representation of the trajectory tracking problem.

where the location of the real mobile robot is denoted as $p = [x \quad y \quad \theta]^T$, $p^{ref} = [x^{ref} \quad y^{ref} \quad \theta^{ref}]^T$ and, v_r^{ref}, v_l^{ref} are the reference trajectory and linear velocities, respectively.

As stated in (5), the control objective is to steer the error, between the desired location and the real location of the mobile robot, close to zero (regulation problem). To express this error with respect to the real robot frame, the following change is considered

$$\begin{bmatrix} e_x(t) \\ e_y(t) \\ e_\theta(t) \end{bmatrix} = \begin{bmatrix} \cos\theta(t) & \sin\theta(t) & 0 \\ -\sin\theta(t) & \cos\theta(t) & 0 \\ 0 & 0 & 1 \end{bmatrix} \cdot \begin{bmatrix} x^{ref}(t) - x(t) \\ y^{ref}(t) - y(t) \\ \theta^{ref}(t) - \theta(t) \end{bmatrix}, \tag{6}$$

where e_x is the longitudinal error, e_y is the lateral error, and e_θ is the orientation error. These errors are graphically presented in Fig. 1 where the *virtual robot* is represented in dotted lines and the real robot in solid ones.

To determine the error along the time, the equation (6) is differentiated producing [13]

$$\dot{e}_x(t) = \alpha(t)e_y(t) + \cos e_\theta(t)\frac{v_r^{ref}(t) + v_l^{ref}(t)}{2} - \frac{v_r(t) + v_l(t)}{2} + \frac{v_r(t)i_r(t) + v_l(t)i_l(t)}{2}$$
$$\dot{e}_y(t) = -\alpha(t)e_x(t) + \sin e_\theta(t)\frac{v_r^{ref}(t) + v_l^{ref}(t)}{2}$$
$$\dot{e}_\theta(t) = \left(\frac{v_r^{ref}(t) - v_l^{ref}(t)}{b} - \frac{v_r(t) - v_l(t)}{b}\right) + \frac{v_r(t)i_r(t) - v_l(t)i_l(t)}{b}, \tag{7}$$

where $\alpha(t) = \left(\frac{v_r(t) - v_l(t)}{b} - \frac{v_r(t)i_r(t) - v_l(t)i_l(t)}{b}\right)$.

In order to linearize the previous equation around the reference trajectory, a first-order Taylor expansion has been used. Furthermore, we have defined the following virtual control signals to eliminate some of the non-linear terms,

$$u_1(t) = \frac{-1 + i_r(t)}{2}v_r(t) + \frac{-1 + i_l(t)}{2}v_l(t) + \frac{v_r^{ref}(t)}{2} + \frac{v_l^{ref}(t)}{2}, \tag{8}$$

$$u_2(t) = \frac{-1 + i_r(t)}{b}v_r(t) + \frac{1 - i_l(t)}{b}v_l(t) + \frac{v_r^{ref}(t)}{b} - \frac{v_l^{ref}(t)}{b}. \tag{9}$$

Afterwards, equation (7) becomes

$$\begin{bmatrix} \dot{e}_x(t) \\ \dot{e}_y(t) \\ \dot{e}_\theta(t) \end{bmatrix} = \begin{bmatrix} 0 & \alpha_r(t) & 0 \\ -\alpha_r(t) & 0 & \dfrac{v_r^{ref}(t)+v_l^{ref}(t)}{2} \\ 0 & 0 & 0 \end{bmatrix} \begin{bmatrix} e_x(t) \\ e_y(t) \\ e_\theta(t) \end{bmatrix} + \begin{bmatrix} 1 & 0 \\ 0 & 0 \\ 0 & 1 \end{bmatrix} \begin{bmatrix} u_1(t) \\ u_2(t) \end{bmatrix}, \tag{10}$$

where

$$\alpha_r(t) = \left(\frac{v_r^{ref}(t) - v_l^{ref}(t)}{b} - \frac{v_r^{ref}(t) i_r(t) - v_l^{ref}(t) i_l(t)}{b} \right).$$

Remark 1: *Notice that the mismatch between the linearized model and the nonlinear system grows for values of e_θ far from 0. It will be shown that, in practice, after the transient, e_θ remains very close to zero. Then, the problem could be present at the first instants, due to the initial condition. For that reason, we assume that, in practice, the real robot and the reference virtual robot start close. In that case, the linearization is successful.*

Equation (10) is expressed in state space representation as a linear, time-varying, continuous-time system

$$\dot{e}(t) = A_{\gamma,c}(t)e(t) + B_c u(t), \tag{11}$$

where $e = [e_x \quad e_y \quad e_\theta]^T$ is the state, $u = [u_1 \quad u_2]^T$ is the (virtual) control input, and γ is the parameter, characterized in Remark 2. Matrices $A_{\gamma,c}$ and B_c are defined as

$$A_{\gamma,c}(t) = \begin{bmatrix} 0 & \alpha_r(t) & 0 \\ -\alpha_r(t) & 0 & \dfrac{v_r^{ref}(t)+v_l^{ref}(t)}{2} \\ 0 & 0 & 0 \end{bmatrix}, \quad B_c = \begin{bmatrix} 1 & 0 \\ 0 & 0 \\ 0 & 1 \end{bmatrix}. \tag{12}$$

Then, the trajectory tracking error model (11) is discretized, obtaining the following linear, time-varying, discrete-time system

$$e(k+1) = A_\gamma(k)e(k) + B_d u(k) \tag{13}$$

where $k \in \mathbb{Z}^+$ is the discrete sample, and matrices A_γ and B_d are now defined as

$$A_\gamma(k) = \begin{bmatrix} 1 & T_m\alpha_r(k) & 0 \\ -T_m\alpha_r(k) & 1 & T_m\dfrac{v_r^{ref}(k)+v_l^{ref}(k)}{2} \\ 0 & 0 & 1 \end{bmatrix}, \quad B_d = \begin{bmatrix} T_m & 0 \\ 0 & 0 \\ 0 & T_m \end{bmatrix}, \tag{14}$$

T_m being the sampling period.

Assumption 1: *Assume that slip factors and reference robot wheel velocities are known at each time and bounded, i.e. $i_r \in [i_r^m, i_r^M]$, $i_l \in [i_l^m, i_l^M]$, $v_r^{ref} \in [v_r^{ref,m}, v_r^{ref,M}]$, and $v_l^{ref} \in [v_l^{ref,m}, v_l^{ref,M}]$.*

Remark 2: *From Assumption 1, we can define a time-varying vector of parameters $\gamma(k) = [v_r^{ref}(k) \quad v_l^{ref}(k) \quad i_r(k) \quad i_l(k)]^T \in \mathbb{R}^4$, and a bounding set $\Gamma \subseteq \mathbb{R}^4$, such that $\gamma(k) \in \Gamma, \forall k \in \mathbb{R}$. For any admissible realization of parameter $\gamma \in \Gamma$, a dynamic matrix denoted as A_γ is determined. Notice that, from Assumption 2, it follows that $A_\gamma \in A$ where A is a polytope in $\mathbb{R}^{3\times 3}$.*

Note that the model is composed by a family of linear systems (defined by matrix A_γ), each of them is controllable provided that $0 \le i_r, i_l < 1$ and $v_r^{ref}, v_l^{ref} > 0$.

For sake of notational simplicity, we omit to express the dependence of $A_\gamma(k)$ on k, employing A_γ to refer to it.

Remark 3: *Note that, according to (8) and (9), the control signals (velocities) are obtained through*

$$v_r(k) = \frac{v_r^{ref}(k) - u_1(k) - \frac{b}{2}u_2(k)}{1 - i_r(k)}, \tag{15}$$

$$v_l(k) = \frac{-v_l^{ref}(k) + u_1(k) - \frac{b}{2}u_2(k)}{-1 + i_l(k)}, \tag{16}$$

where $v_r \in [v_r^m, v_r^M]$ and $v_l \in [v_l^m, v_l^M]$.

As commented above, states and inputs of the system are subject to constraints, that is

$$e(k) \in E, \quad u(k) \in U, \tag{17}$$

where $E \subseteq \mathbb{R}^3$ and $U \subseteq \mathbb{R}^2$ are polytopes and contain the origin.

Remark 4: *Note that, equations (15) and (16) lead to bounds on the space of u, obtained from the constraints on* $v_r, v_l, i_r, i_l, v_r^{ref}, v_l^{ref}$.

3. Adaptive Control Using Linear Matrix Inequalities

LMI are known as an efficient tool for solving convex optimization problems. LMI have an extensive application in the field of automatic control involving robust and optimal control [5, 14, 17, 24].

A linear matrix inequality is a matrix inequality of the form [5]

$$F(x) = F_0 + \sum_{i=1}^{m} x_i F_i > 0, \tag{18}$$

where $x \in \mathbb{R}^m$ is the decision variable and the symmetric matrices $F_i = F_i^T \in \mathbb{R}^{n \times n}$, $i = 0, \ldots, m$, are given. The inequality $F(x) > 0$ means that $F(x)$ is positive-definite. For a complete description of LMI, see [5] and the references therein.

Now, we pose the trajectory tracking control problem in terms of an LMI optimization problem, in order to obtain a positive definite matrix P determining a Lyapunov function and a set of feedback gains which provide the control law. This problem is solved off-line considering all the extreme realizations of the parameter. Afterwards, an adaptive feedback control law is obtained on-line depending on the current realization of the parameter γ, which is obtained as a convex combination of the extremal feedback gains.

The control scheme implemented in this paper is summarized in Fig. 2. The adaptive controller uses an estimation of the slip and the reference to determine the feedback gain guaranteeing asymptotic stability.

The control strategy is designed to satisfy different specifications, in particular, it is required to provide:

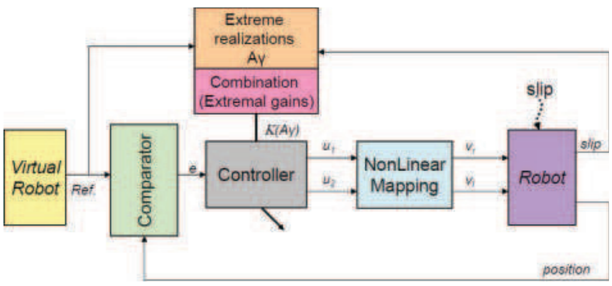

Fig. 2. Control scheme for the adaptive control strategy.

- Input and state constraints fulfillment: this requirement is guaranteed through the determination of an invariant set [2], i.e. a set in the state space in which the system state can be confined by the control law. An ellipsoidal invariant set is computed ensuring constraints satisfaction and providing a feasibility region for the controller.
- Asymptotic stability: it is achieved by means of a quadratic Lyapunov function, i.e. a positive definite function decreasing along the trajectories of the closed-loop system.
- Performance: the quadratic Lyapunov function provides an upper bound on the cost-to-go as close as possible to the optimal LQR cost. We recall that, with cost-to-go, we consider the sum of the stage cost, from the present to the infinite time. Our solution provides a cost-to-go function which is an overbound of the optimal LQR one. The objective of the optimization problem is to minimize such overbounding function, to make the cost-to-go as close as possible to the optimal one, i.e. the LQR cost.
- Adaptivity: the control has to fulfill the specifications for any of the admissible realization of the parameter in the bounded set Γ. For that reason, a feedback gain is designed for any extremal realization of the linear system, such that the quadratic function is a common Lyapunov function. The set of controllers induces a time-varying feedback gain.
- Performance region: we define a target set of the state space where the performance is considered. The objective is that the controller obtained solving LMI has higher performance inside this set, which is the region of the state space in which the system is confined in practice.
- Fast real-time implementation: once the feedback gains have been calculated for each extremal parameter realization, it is sufficient to solve on-line a linear programming problem to obtain the stabilizing control law. This fact supposes that the presented control strategy fits very well to mobile robotic applications, where small sampling rates are employed.

Given a linear, time-varying, discrete-time system in the form (13) and subject to the constraints (17), we look for a matrix $P > 0$ and a set of parameter-dependent controllers $K(A_\gamma^j)$, one for each vertex γ^j of Γ, such that for all $e \in \varepsilon(P)$ the system is asymptotically stable, and the input and state constraints are fulfilled.

Note that, in order to assure the stated specifications, it is required that the state evolves inside an invariant set $\varepsilon(P)$, i.e., $e \in \varepsilon(P) = \{e \in \mathbb{R}^3 : e^T P e \leq 1\}$. In our case, invariance is assured by the fact that the ellipsoid is a level set of a Lyapunov function. This region has the property that if the initial state belongs to it, all the following states are contained in that set for any possible realization of the parameter [2].

Remark 5: *In the following, all the conditions required are imposed only at the extremal values of the polytopic set Γ, i.e. at the N_γ vertices of Γ. In our case, $N_\gamma = 2^4$, as shown in Assumption 1, matrix A_γ is determined by the admissible realization of four variables $(v_r^{ref}, v_l^{ref}, i_r, i_l)$. Fulfillment of such conditions at the vertices yields the satisfaction at any point in Γ, as stated in Property 1, that will be presented in Section III-E.*

In the following section, we detail the design of the control strategy used in this work to assure previous specifications, regarding adaptivity and constraints fulfillment.

3.1. Stability and Performance

When dealing with the problem of determining asymptotically stable controllers, one classical way to proceed is to look for a Lyapunov function determined by a positive definite matrix $P > 0$, i.e. $V(e) = e^T Pe$, such that $V(e(k+1)) - V(e(k)) < 0$, for all $e \neq 0$ [5, 17]. In general, invariant ellipsoid and Lyapunov function are both determined by P. We add a further degree of freedom introducing a scaling factor in the definition of the Lyapunov function $V(e) = e^T \mu Pe, \mu \in \mathbb{R}^+$.

The value of variable μ is minimized in the optimization problem (see (40)). It is shown in Remark 6 that the value of μ provides an upper bound of the cost-to-go valid within the performance region. Hence, conceptually, minimizing μ implies maximizing the performance in the region of interest (defined in Section III-D).

As explained previously, the LMI to be solved is formulated as

$$\begin{aligned} &e^T((A_\gamma^j + B_d K(A_\gamma^j))^T \mu P(A_\gamma^j + B_d K(A_\gamma^j)))e - e^T(\mu P)e \\ &\leq -e^T(Q + K(A_\gamma^j)^T RK(A_\gamma^j))e, \quad \forall e \in \mathbb{R}^3, \end{aligned} \tag{19}$$

for every vertex γ^j of Γ, with $j = 1, \ldots, N_\gamma$, where $Q > 0$, $R > 0$ are symmetric matrices weighting the state and input signals. Notice that inequality (19) gives a guaranteed cost function, for details see [17].

Denoting $\bar{A}_\gamma^j = A_\gamma^j + B_d K(A_\gamma^j)$, we get

$$\begin{aligned} &e^T((\bar{A}_\gamma^j)^T \mu P(\bar{A}_\gamma^j))e - e^T(\mu P)e \leq \\ &- e^T(Q + K(A_\gamma^j)^T RK(A_\gamma^j))e, \quad \forall e \in \mathbb{R}^3, \end{aligned} \tag{20}$$

for all γ^j, with $j = 1, \ldots, N_\gamma$. The previous inequality is equivalent to the following LMI

$$(\bar{A}_\gamma^j)^T \mu P(\bar{A}_\gamma^j) - \mu P \leq -Q - K(A_\gamma^j)^T RK(A_\gamma^j), \tag{21}$$

for all γ^j, with $j = 1, \ldots, N_\gamma$. Using the Schur complement [5], it results that the previous inequality is equivalent to

$$\begin{bmatrix} P - \dfrac{Q}{\mu} - K(A_\gamma^j)^T \dfrac{R}{\mu} K(A_\gamma^j) & (\bar{A}_\gamma^j)^T \\ \bar{A}_\gamma^j & P^{-1} \end{bmatrix} \geq 0, \tag{22}$$

for all γ^j. Rearranging the previous LMI, we obtain

$$\begin{bmatrix} P & (\bar{A}_\gamma^j)^T & Q^{\frac{1}{2}} & K(A_\gamma^j)^T R^{\frac{1}{2}} \\ \bar{A}_\gamma^j & P^{-1} & 0 & 0 \\ Q^{\frac{1}{2}} & 0 & \mu I & 0 \\ R^{\frac{1}{2}} K(A_\gamma^j) & 0 & 0 & \mu I \end{bmatrix} \geq 0, \tag{23}$$

for all γ^j. In order to remove the nonlinear terms on P, the previous matrix inequality is pre- and post-multiplied by

$$\begin{bmatrix} P^{-1} & 1 & 0 & 0 \\ 0 & I & 0 & 0 \\ 0 & 0 & I & 0 \\ 0 & 0 & 0 & I \end{bmatrix}. \tag{24}$$

Finally, substituting $S = P^{-1}$, $Y_\gamma^j = K(A_\gamma^j)P^{-1}$, and $\bar{A}_\gamma^j = A_\gamma^j + B_d K(A_\gamma^j)$, the linear matrix inequality to solve is given by

$$\begin{bmatrix} S & S(A_\gamma^j)^T + (Y_\gamma^j)^T B_d^T & SQ^{\frac{1}{2}} & (Y_\gamma^j)^T R^{\frac{1}{2}} \\ (A_\gamma^j)S + B_d(Y_\gamma^j) & S & 0 & 0 \\ Q^{\frac{1}{2}} S & 0 & \mu I & 0 \\ R^{\frac{1}{2}} Y_\gamma^j & 0 & 0 & \mu I \end{bmatrix} \geq 0, \tag{25}$$

for all γ^j. This LMI is imposed for each vertex of the set Γ, and the solution of the optimization problem determines a feedback gain for each vertex. For that reason, we determine off-line $N_\gamma = 2^4$ control gains.

3.2. Input Constraints

Physical limitations in the actuators of the mobile robot impose constraints on the input variables. We have to impose, in LMI form, that no point of the invariant ellipsoid causes input constraint violations.

Knowing that $v_r \leq v_r^M$ and $v_l \leq v_l^M$, we find that such restriction in terms of the virtual control inputs is[1]

$$\left(\frac{v_r^{ref} - u_1 - \frac{b}{2}u_2}{1 - i_r} \right) \leq v_r^M, \tag{26}$$

we formulate the LMI for the case of v_r, the case for v_l is obtained in a similar way.

Now, rearranging equation (26), we get

$$C_\gamma^j u + d_\gamma^j \leq v_r^M, \tag{27}$$

for all γ^j, where $C_\gamma^j = \left[\frac{-1}{1 - i_r} \quad \frac{-b}{2(1 - i_r)} \right]$, $d_\gamma^j = \frac{v_r^{ref}}{1 - i_r}$ and clearly, i_r and v_r^{ref} are those related to the particular extremal realization γ^j of the parameter.

Defining $\eta_\gamma^j = v_r^M - d_\gamma^j$ and substituting $u = K(A_\gamma^j)\, e$, previous inequality becomes

$$C_\gamma^j K(A_\gamma^j) e \leq \eta_\gamma^j, \quad \forall e \in \varepsilon(P), \tag{28}$$

for all γ^j. Considering the following problem to determine the maximum of a linear function with ellipsoidal constraints, i.e.

$$a^* = \max_e \quad C_\gamma^j K(A_\gamma^j)\boldsymbol{e} \quad s.t. \qquad e^T P e \leq 1, \tag{29}$$

the solution to the previous maximization problem is (see [5])

$$a^* = \sqrt{C_\gamma^j K(A_\gamma^j) P^{-1} (K(A_\gamma^j))^T (C_\gamma^j)^T}. \tag{30}$$

Hence, a necessary and sufficient condition for (28) to be fulfilled is that

$$C_\gamma^j K(A_\gamma^j) P^{-1} (K(A_\gamma^j))^T (C_\gamma^j)^T \leq (\eta_\gamma^j)^2, \tag{31}$$

for all γ^j. Notice that a quadratic term $(\eta_\gamma^j)^2$, depending on γ^j appears. In order to assure the convexity properties of LMI, it should be substituted for the upper bound $\bar{\eta} = v_r^M - \frac{v_r^{ref,M}}{1 - i_r^M}$. Thus, it produces

$$C_\gamma^j K(A_\gamma^j) P^{-1} (K(A_\gamma^j))^T (C_\gamma^j)^T \leq (\bar{\eta})^2, \tag{32}$$

for all γ^j. Then, applying the Schur complement, it becomes

[1] Notice that, in practice, the wheels can also move backward. However, these negative velocities are rarely reached, as the reference virtual robot always moves forward and for that reason no lower bounds have to be added to the optimization problem.

$$\begin{bmatrix} (\bar{\eta})^2 & C_\gamma^j K(A_\gamma^j) \\ (K(A_\gamma^j))^T (C_{\gamma^j})^T & P \end{bmatrix} \geq 0, \tag{33}$$

for all γ^j. Finally, previous equation is pre- and post-multiplied by

$$\begin{bmatrix} I & 0 \\ 0 & P^{-1} \end{bmatrix}, \tag{34}$$

and substituting $S = P^{-1}$ and $Y_\gamma^j = K(A_\gamma^j) P^{-1}$, the input constraints result in the following LMI form

$$\begin{bmatrix} (\bar{\eta})^2 & C_\gamma^j Y_\gamma^j \\ (Y_\gamma^j)^T (C_\gamma^j)^T & S \end{bmatrix} \geq 0, \tag{35}$$

for every vertex γ^j of Γ, with $j = 1, \ldots, N_\gamma$.

3.3. State constraints

In addition, we have to impose that the invariant set is contained in the admissible state space region. This guarantees no state constraint violations, provided that the initial state is confined in $\varepsilon(P)$. In this way, state constraints are formulated as

$$|e| \leq T, \quad \forall e \in \varepsilon(P), \tag{36}$$

where $|\cdot|$ denoted the element-wise absolute value and $T = [e_x^M \quad e_y^M \quad e_\theta^M]^T$.

Similarly to the case of input constraints, and substituting $S = P^{-1}$, it produces

$$\begin{aligned} h_1^T S h_1 &\leq (e_x^M)^2, \\ h_2^T S h_2 &\leq (e_y^M)^2, \\ h_3^T S h_3 &\leq (e_\theta^M)^2, \end{aligned} \tag{37}$$

where $h_1 = [1\ 0\ 0]^T$, $h_2 = [0\ 1\ 0]^T$, and $h_3 = [0\ 0\ 1]^T$. Finally, due to symmetry of LMI, this equation is also achieved for the lower bounds.

3.4. Performance Region

We establish a target region, denoted as Ψ, which can be considered as a performance region, in which the system evolves mostly. The objective is that the controller obtained solving LMI has higher performance inside this set. We define $\psi_e^j \in \Psi$ as the j-th vertex of Ψ. The set Ψ is the parallelotope in the state space determined by the intervals of interest, i.e. $\Psi = \{e : \psi^m \leq e \leq \psi^M\}$, and we impose $\Psi \subseteq \varepsilon(P)$.

In LMI form, it must be imposed that all the vertices of Ψ belong to the invariant ellipsoid, i.e.

$$1 - (\psi_e^j)^T P(\psi_e^j) \geq 0, \tag{38}$$

which is equivalent to

$$\begin{bmatrix} 1 & (\psi_e^j)^T \\ \psi_e^j & S \end{bmatrix} \geq 0. \tag{39}$$

In conclusion, the off-line design process is aimed to obtain a family of control gains fulfilling the LMI constraints. These gains are obtained solving the following optimization problem.

$$\begin{aligned} &\min_{S>0,\mu,\,Y_\gamma^j\forall\gamma^j} \quad \mu \\ &s.t. \\ &\qquad (25), (35), (37),\ \forall\gamma^j, \\ &\qquad\qquad (39),\ \forall\psi_e^j. \end{aligned} \tag{40}$$

Remark 6: *We provide here an explanation of the meaning of parameter μ, whose minimization is the objective of the proposed optimization problem. We will show that the value of μ is an upper bound of the cost-to-go, at least within the performance region represented by Ψ.*

First, we suppose that the performance region is contained in the ellipsoidal invariant set, imposing that every vertex of Ψ is contained in the ellipsoid through constraint (38).

Moreover, it can be proved that, from the constraint (19), the quadratic function $V(e) = e^T\mu Pe$ is an upper bound of the cost-to-go function, see Property 1. Then, for every $e(0) \in \varepsilon(P)$, the upper bound of the cost-to-go is given by

$$V(e(0)) = e^T(0)\mu Pe(0) \leq \mu, \tag{41}$$

as $e^T(0)Pe(0) \leq 1$ by definition of the ellipsoid $\varepsilon(P)$. This implies that also the value of μ is an upper bound of the cost-to-go valid for every point in the ellipsoid $\varepsilon(P)$, and in particular in the region Ψ. That is, the cost-to-go of the resulting adaptive control law is smaller or equal to μ, for every initial condition in Ψ. Hence, minimizing the value of μ, we minimize an upper bound of the cost-to-go valid for every point in the performance region.

Fig. 3 plots the invariant ellipsoid obtained solving (40) using the LMI toolbox [11] and MPT toolbox [18] both for Matlab® Suite. The small box inside the ellipsoid depicts the set Ψ. As expected, the ellipsoid is constrained by the performance region. Furthermore, input and state constraints are also drawn, the values of these constraints are also employed in the simulations, see Table 1. Recall that, once the feedback law is defined, the input constraints are projected into the state space (see (28)). This can be noticed in the top right cuts of the outer box in Fig. 3.

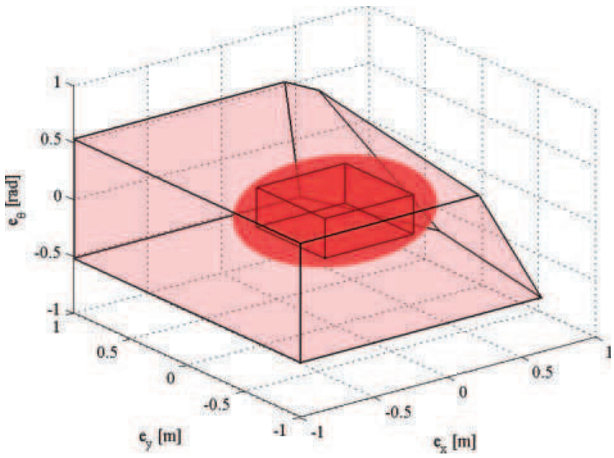

Fig. 3. Ellipsoidal invariant set, input and state constraints, and performance region.

Table 1. Input and state constraints, and performance region for simulations

	Max	Min	Units
Input			
v_r	2.5	0	[m/s]
v_l	2.5	0	[m/s]
State			
e_x	1	− 1	[m]
e_y	1	− 1	[m]
e_θ	0.52	− 0.52	[rad]
Performance region			
ψ_{e_x}	0.3	− 0.3	[m]
ψ_{e_y}	0.3	− 0.3	[m]
ψ_{e_θ}	0.17	− 0.17	[rad]

3.5. On-line Adaptive Control Strategy

Finally, in order to assure the performance and stability of the gain determined on-line (adaptive controller), we have to compute a vector of coefficients $\lambda \in \mathbb{R}^{N_\gamma}$ such that A_γ is a convex combination of the extreme matrices of the set A. For that purpose, we can express

$$\begin{aligned} A_\gamma &= \sum_{j=1}^{N_\gamma} \lambda_j A_\gamma^j, \\ &\sum_{j=1}^{N_\gamma} \lambda_j = 1, \quad \lambda_j \geq 0, \quad \forall j = 1, \ldots, N_\gamma, \end{aligned} \tag{42}$$

where A_γ is the current matrix (on-line).

The problem to determine λ is a Linear Programming (LP) feasibility problem with respect to λ, that is, we only need to find a feasible solution to equation (42).

Then, the proposed adaptive feedback gain for the current realization state is calculated as

$$K(\mathcal{A}) = \lambda_1 K(A_\gamma^1) + \ldots + \lambda_{N_\gamma} K(A_\gamma^{N_\gamma}). \tag{43}$$

Finally, the resulting feedback control law is

$$u(k) = K(A_\gamma)e(k). \tag{44}$$

In the following property, we establish that adaptive control law (44) assures the specifications given in Section 3 for any $A_\gamma \in A$.

Property 1: Suppose that Assumption 1 holds. Consider the linear, time-varying, discrete-time system (13) with constraints $e(k) \in E$, $u(k) \in U$. The adaptive control law defined in (44), is such that, for each $\gamma \in \Gamma$:

- The function $V(e) = e^T \mu P e$ is a local Lyapunov function for the system inside $\varepsilon(P) = \{e : e^T P e \leq 1\}$ ensuring stability.
- The set $\varepsilon(P) = \{e : e^T P e \leq 1\}$ is an invariant set for the closed-loop system satisfying input and state constraints.
- The function $V(e)$ is an upper bound of the cost-to-go, and of the cost of the LQR, i.e.,

$$V(e(0)) \geq \min_{u_{[0,\infty)}} \sum_{k=0}^{\infty} e^T(k) Q e(k) + u(k)^T R u(k), \tag{45}$$

where $u_{[0,\infty)}$ denotes the infinite sequence of $u(k)$ for $k \in \mathbb{Z}^+$ and $\forall e \in \varepsilon(P)$. The proof can be found in Appendix A.

4. Simulations

This section analyzes the performance of the proposed adaptive control law, and it provides a comparison with existing time-varying control techniques. For this purpose, the well-known linear, time-varying controller described in [8] has been implemented. Furthermore, in order to compare our new formulation with a controller that compensates slip effect, the control law presented in [13] has also been implemented.

Although, many different trajectories have been tested, in this case, we show a reference trajectory, which is not too typical in mobile robotics, but it has been included in order to check the full velocity and slip ranges. In order to make realistic simulations, we have added a small random noise to the measurements of the robot position and to the slips. The initial location of the mobile robot is also different from the desired one. The parameters of the controllers developed in [8, 13] are set to $\beta = 1$ and $\delta = 0.6$ in order to reach a soft overdamped closed-loop behavior, see [8,13] for more details. The rest of parameters are: $T_m = 0.1[s]$, $b = 0.5[m]$ and the parameters for the proposed adaptive control law are $Q = diag([1 \quad 1 \quad 0.1])$ and $R = 10I_2$. Reference velocities are restricted to $\{v_r^{ref}, v_l^{ref} \in [0.4, 1.5][m/s]\}$ and slip is restricted to $\{i_r, i_l \in [10, 30][\%]\}$. The state and input constraints are summarized in Table 1.

Fig. 4a shows the trajectories. It is possible to observe that the control laws, which take into account slip effect, have a better behavior than the controller proposed in [8]. In Fig. 4b, we notice that the simulated slip varies over the whole range previously defined. The errors between the reference trajectory and those steered by the compared controllers are plotted in Fig. 5. As expected, the controller presented in this

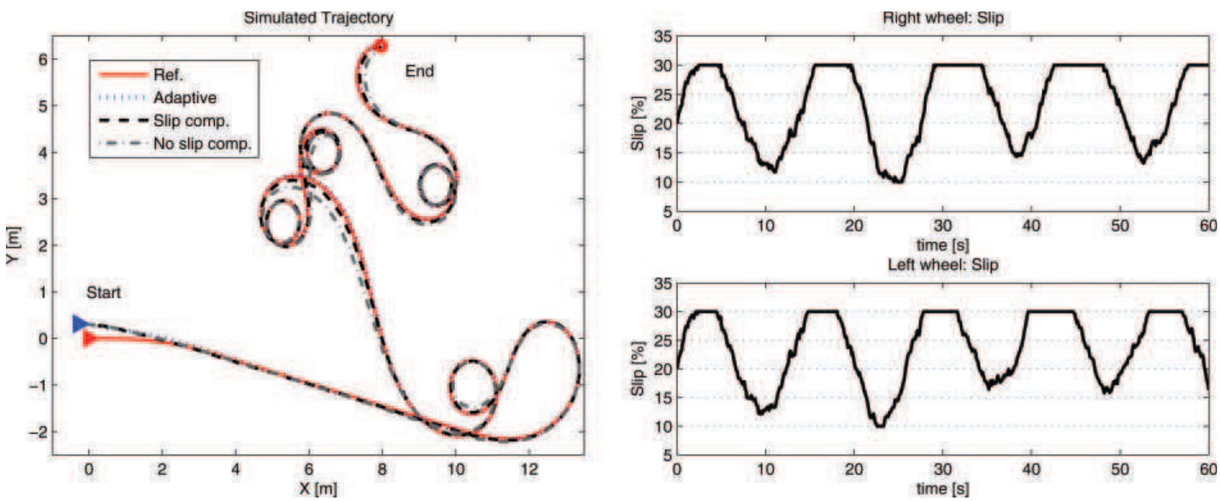

Fig. 4. Simulated trajectories and Slip.

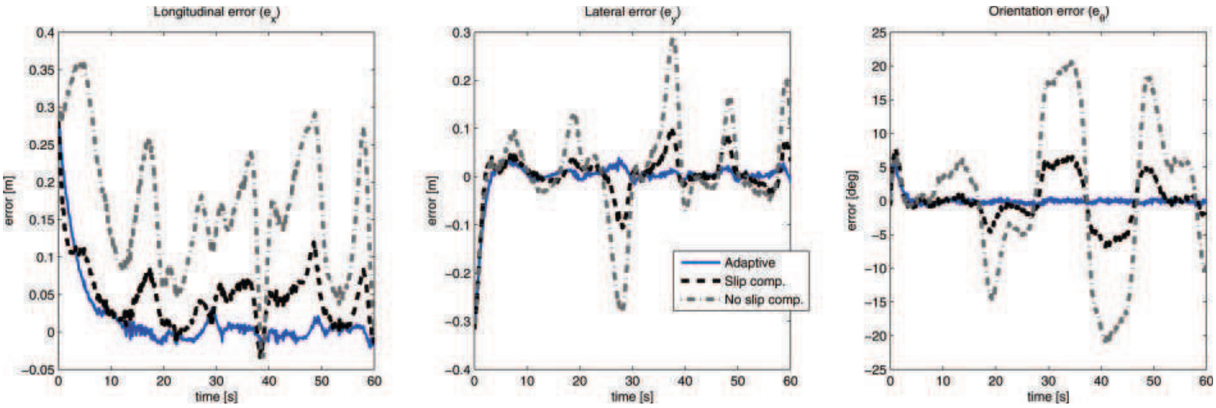

Fig. 5. Errors along the simulations.

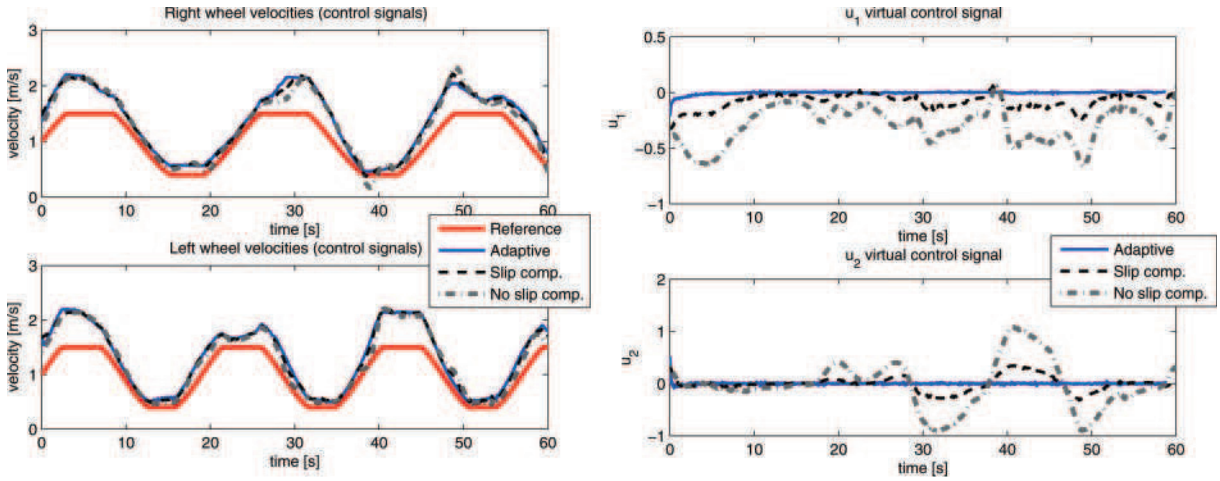

Fig. 6. Control and virtual signals along the simulations.

work achieves the smallest error due to the adaptivity of the control law for each reference inside the specifications. It is possible to note that although some noise has been added to the slip and the robot position, the adaptive control law obtains the smallest error mainly in the lateral direction. Large lateral errors could cause crashes with obstacles in its workspace. In the proposed controller, it is assured that lateral errors are always smaller than in the other cases.

As explained above, longitudinal slip decreases the linear velocity, which means that controllers must increase this component of the velocity to compensate this negative effect. For that reason, the velocities displayed in Fig. 6a are greater than the references. Finally, Fig. 6b shows the virtual control signals for the three controllers. The adaptive controller presents control signals, which are much smoother than the other control laws.

5. Conclusions

This paper presents the synthesis of an adaptive control law guaranteeing asymptotic stability for mobile robots under slip conditions subject to both constraints and varying dynamics. LMI are used to solve this convex optimization problem. This problem is solved off-line for each extreme system realization. On-line computation is devoted to determine an adaptive feedback control law for the current realization of the system as a convex combination of the extremal gains obtained off-line. Finally, a comparative study with other control laws have been addressed through simulations. These simulations show the appropriate behavior of the proposed formulation, state and input constraints are assured, and longitudinal slip is compensated. In future, we are planning to test this control strategy in a real mobile robot.

Acknowledgments

This work has been supported by the Spanish CICYT under grants DPI 2007-66718-C04-01 and DPI 2007-66718-C04-04.

References

1. Bigras, P, Petrov P, Wong T. A LMI approach to feedback path control for an articulated mining vehicle, IMACS Electrimacs, Montreal, Canada, 2002
2. Blanchini F. Set invariance in control. *Automatica* 1999; 35(11): 1747–1767
3. Blanchini F, Miani S. Set-Theoretic Methods in Control. Birkhäuser, Boston, USA, 2007
4. Bloch A, McClamroch N. Control of mechanical systems with classical nonholonomic constraints. In: IEEE Conference on Decision and Control, Tampa, USA, 1989, pp. 201–205
5. Boyd S, El Ghaoui L, Feron E, Balakrishnan V. Linear Matrix Inequalities in System and Control Theory. Society for Industrial and Applied Mathematics, Philadelphia, USA, 1994
6. Brockett R. Asyptotic Stability and Feedback Stabilization. Differential Geometric Control Theory. Birkhauser, USA, 1983
7. Campion G, Bastin G, D'Andréa-Novel B. Structural properties and classification of kinematic and dynamic models of wheeled mobile robots. *IEEE Trans Robotics Autom* 1996; 12(1): 47–62
8. Canudas C, Siciliano B, Bastin G, Theory of Robot Control. Springer, The Netherlands, 1997
9. Chang YC, Chen BS. Adaptive tracking control design of constrained robot systems. *Int J Adaptive Control Signal Proc* 1998; 12(6): 495–526
10. Fang H, Fan R, Thuilot B, Martinet P. Trajectory tracking control of farm vehicles in presence of sliding. *Robotics Autonomous Syst* 2006; 54(10): 828–839
11. Gahinet P, Nemirovski A, Laub AJ, Chilali M. LMI Control Toolbox User's Guide. The MathWorks, Inc., USA, 1995
12. Ghabcheloo R, Pascoal A, Silvestre C, Kaminer I. Nonlinear co-ordinated path following control of multiple wheeled robots with bidirectional communication constraints. *Int J Adaptive Control Signal Proc* 2007; 21(2): 133–157
13. Gonzalez R, Rodriguez F, Guzman JL, Berenguel M. Localization and control of tracked mobile robots under slip conditions. In: IEEE International Conference on Mechatronics, Málaga, Spain, 2009
14. Guzman JL, Alamo T, Berenguel M, Dormido S, Camacho EF. A robust constrained reference governor approach using linear matrix inequalities. *J Proc Control* 2009; 19(5): 773–784
15. Kitano M, Kuma M. An analysis of horizontal plane motion of tracked vehicles. *J Terramech* 1977; 14(4): 211–225
16. Klančar G, Škrjanc, I. Tracking-error model-based predictive control for mobile robots in real time. *Robotics Autonom Syst* 2007; 55(1): 460–469
17. Kothare MV, Balakrishnan V, Morari M. Robust constrained model predictive control using linear matrix inequalities. *Automatica* 1996; 32(10): 1361–1379
18. Kvasnica M, Grieder P, Baotić M. Multi-Parametric Toolbox (MPT). Available online: http://control.ee.ethz.ch/mpt, 2004
19. Le A. Modelling and control of tracked vehicles, Ph.D. Thesis, University of Sydney, Sydney, Australia, 1999
20. Lee TC, Chen BS, Chang YC. Adaptive control of robots by linear time-varying dynamic positon feedback. *Int J Adaptive Control Signal Proc* 1996; 10(6): 649–671
21. Lenain R, Thuilot B, Cariou C, Martinet P. Adaptive and predictive path tracking control for off-road mobile robots. *Eur J Control* 2007; 13(4): 419–439
22. Martínez JL, Mandow A, Morales J, Pedraza S, García-Cerezo A. Approximating kinematics for tracked mobile robots. *Int J Robotics Res* 2005; 24(10): 867–878
23. Masehian E, Habibi G. Motion planning and control of mobile robot using linear matrix inequalities. In: IEEE International Conference on Intelligent Robots and Systems, San Diego, USA, 2007, pp. 4277–4282
24. Peaucelle D, Khan HM, Pakshin P. LMI-based analysis of robust adaptive control for linear systems with time-varying uncertainty. Automation and Remote Control, submitted in november 2008, to appear
25. Pourboghrat F, Karlsson M.P. Adaptive control of dynamic mobile robots with nonholonomic constraints. *Computers Electrical Eng* 2002; 28(4): 241–253
26. Samson C, Ait-Abderrahim K. Feedback stabilization of a nonholonomic wheeled mobile robot. In: IEEE Workshop on Intelligent Robots and Systems. Osaka, Japan, 1991, pp 1242–1247.
27. Shiller Z, Serate W, Hua M. Trajectory planning of tracked vehicles. *J Dynamic Syst Measure Control* 1995; 117: 619–624
28. Siegwart R, Nourbakhsh I. Introduction to Autonomous Mobile Robots. A Bradford book. The MIT Press, USA, 2004
29. Tanaka K, Kosaki T, Wang HO. Backing control problem of a mobile robot with multiple trailers: Fuzzy modeling and LMI-based design. *IEEE Trans Syst Man Cybernetics* 1998; 28(3): 329–337
30. Wang W, Low CB. Modeling and analysis of skidding and slipping in wheeled mobile robots: Control design perspective. *IEEE Trans Robotics* 2008; 24(3): 676–687
31. Wong JY. Theory of Ground Vehicles. John Wiley and Sons, USA, 2001
32. Yang TT, Liu ZY, Chen H, Pei R. The research on robust tracking control of constrained wheeled mobile robots. In: IEEE International Conference on Machine Learning and Cybernetics, Guangzhou, Japan, 2005, pp 1356–1361

Appendix

Proof of Property 1

In the following, we assume that λ are obtained such that A_γ is a convex combination of A^j_γ, with γ^j the N_γ vertices of Γ as in (19) and $K(A_\gamma)$ is determined as in (43). The three statements of the property are proved.

We start proving the third point, as the first one is a direct consequence of it.

To prove the third point, we have to show that inequality,

$$e^T((A_\gamma + B_d K(A_\gamma))^T \mu P(A_\gamma + B_d K(A_\gamma)))e - e^T(\mu P)e \\ \leq -e^T(Q + K(A_\gamma)^T R K(A_\gamma))e, \quad \forall e \in R^3, \tag{46}$$

is satisfied for any $\gamma \in \Gamma$ if it is satisfied at the vertices γ^j, with $j = 1, \ldots, N_\gamma$. To simplify the notation, we define

$$M_\gamma = \begin{bmatrix} S & S(A_\gamma)^T + (Y_\gamma)^T B_d^T & SQ^{\frac{1}{2}} & (Y_\gamma)^T R^{\frac{1}{2}} \\ (A_\gamma)S + B_d(Y_\gamma) & S & 0 & 0 \\ Q^{\frac{1}{2}} S & 0 & \mu I & 0 \\ R^{\frac{1}{2}} Y_\gamma & 0 & 0 & \mu I \end{bmatrix}, \tag{47}$$

where the dependence on the parameter γ is explicit, and note that $M_\gamma = \sum_{i=1}^{N_\gamma} \lambda^j M_{\gamma^j}$. Since, as illustrated in Subsection III-A, condition (46) is equivalent to $M_\gamma \geq 0$, and from (25) and the non-negativeness of λ, we have that

$$M_\gamma = \sum_{i=1}^{N_\gamma} \lambda^j M_{\gamma^j} \geq 0, \tag{48}$$

it means that (46) is fulfilled. To prove that $V(e)$ is a Lyapunov function for the closed-loop system regardless of the realization of parameter γ, we have to show that for any $\gamma \in \Gamma$ condition $V(e(k+1)) - V(e(k)) < 0$ is satisfied, i.e.,

$$e^T((A_\gamma + B_d K(A_\gamma))^T \mu P(A_\gamma + B_d K(A_\gamma))) \\ e - e^T(\mu P)e < 0, \quad \forall e \in \mathbb{R}^3, \tag{49}$$

as $V(e)$ is positive definite. From $Q > 0$, $R > 0$ and (46), the condition follows. Furthermore, since we prove it for the entire space, $V(e)$ is, in particular, a Lyapunov function in the ellipsoid centered in the origin. Finally, the set $\varepsilon(P)$ is an invariant set, since it is the level set of a Lyapunov function (see [3]), and it fulfills the state constraints by construction. With respect to the input constraints, we have that

$$C_\gamma K(A_\gamma)e = \sum_{j=1}^{N_\gamma} \lambda^j C_{\gamma^j} K(A_\gamma^j)e \leq \sum_{i=1}^{N_\gamma} \lambda^j \bar{\eta} = \bar{\eta} \\ \forall e \in \varepsilon(P), \tag{50}$$

is satisfied by convexity of Γ and fulfillment of input constraints at its vertices.■